Spectroscopic and Photophysical Properties of Thiophene−Fluorene Oligomers as well as Their Corresponding Polyesters

Michel Belletête,[†] Jean-Francois Morin,[‡] Serge Beaupré,[‡] Maxime Ranger,[‡] Mario Leclerc,[‡] and Gilles Durocher*[,†]

Laboratoire de photophysique moléculaire, Département de Chimie, Université de Montréal, C.P. 6128, Succ. Centre-Ville, Montréal, Québec, H3C 3J7, Canada; and Laboratoire des polymères photoactifs et électroactifs, Centre de recherche en sciences et ingénierie des macromolécules (CERSIM), Université Laval, Cité Universitaire, Québec, G1K 7P4, Canada

Received June 15, 2000; Revised Manuscript Received December 11, 2000

ABSTRACT: A study of the spectroscopy and photophysics of thiophene−fluorene oligomers as well as the respective molecules incorporated in polyesters are reported. The same oligomers having carbonyl groups at both ends of the molecules have also been studied. These molecules provide a better correlation with their corresponding polyesters. The first absorption band of each derivative can be assigned to the $S_1 \leftarrow S_0$ electronic transition computed from ZINDO/S calculations performed on the optimized geometries (HF/6-31G*). This transition corresponds mainly to the promotion of an electron from the HOMO to the LUMO and is strongly allowed and polarized along the long axis of the molecular frame. The insertion of alkyl lateral chains at the 3-position of the thiophene rings caused a torsion of the backbone of the oligomers, which induces a blue shift of the absorption band. From fluorescence data, it is observed that a more planar conformation is favored in the relaxed excited states. The increase of the oligomer chain or the addition of carbonyl groups at both ends of the molecules induces a red shift of the spectra due to an increase in the electronic delocalization along the molecular frame. It was shown by HF/6-31G* ab initio calculations that the length of the oligomer chain and/or the presence of carbonyl groups do not significantly influence the ground state molecular conformation. In the polyesters, thiophene−fluorene units have about the same spectral positions as those of the corresponding esters indicating that the oligomers are well isolated in the polyester chain. Fluorescence quantum yields and lifetimes of methyl-substituted derivatives are smaller than those of the unsubstituted molecules. Similarly, these photophysical parameters are smaller for the polyesters compared to those of the respective esters. In these systems, the photophysical properties are mainly governed by nonradiative processes. However the luminescence of the polyesters remains relatively intense making them suitable for LED materials.

1. Introduction

Conjugated polymers and oligomers have been investigated intensively in the past few decades because of their unusual electrical and optical properties, making them applicable to electronic and photonic devices such as field-effect transistors[1,2] and light-emitting diodes (LED).[3−10] Among these materials, oligothiophenes are of special interest. Indeed, by increasing the repeat units in the molecules and/or by adding side chains on thiophene rings, oligothiophenes permit color tuning.[11−19] The incorporation of thiophene derivatives with different ring numbers in polyesters presents an interesting alternative to tunable light-emitting materials. Recently, blue-light emitting materials derived from oligothiophenes incorporated in polyesters have been obtained and characterized.[20−22] Unfortunately, these materials have weak fluorescence quantum yields putting some limitations on their use in optical devices.

Fully conjugated polyfluorenes have been studied recently for LED applications[23−26] because fluorene derivatives are highly fluorescent compounds[27−30] with facile functionalization at the C-9 position permitting to control the polymer solubility by adding alkyl chains. However, some of these fully conjugated polymers form excimers which may limit their utilization in optical devices. The incorporation of fluorene derivatives in polyesters might solve this problem. These polyesters are particularly interesting since they combine the good mechanical properties and processability of high molecular weight polymers to the electrical and optical properties of the oligomers. Along these lines, we have recently shown that a terfluorene incorporated in a polyester does not show any formation of excimers whereas its optical properties are very close to that of the isolated molecule.[29] Moreover the luminescence intensity of the polyester remains quite intense thus showing promising optical features for LED applications. From these encouraging results, we have decided to develop a new class of tunable emissive polyesters derived from thiophene−fluorene and phenylene−fluorene oligomers. Therefore, we report herein the optical properties and photophysics of 2,7-bis(2-thienyl)-9,9-dioctylfluorene (TFT), 2,7-bis(3-methylthien-2-yl)-9,9-dioctylfluorene (MTFMT), and 2,7-bis(2,2′-bithien-5-yl)-9,9-dioctylfluorene (BTFBT) in solution as well as incorporated in a polyester. The results are discussed in terms of both the steric hindrance between adjacent rings and the conjugation length. To correlate the spectroscopic and photophysics of the polyesters with those of the respective oligomers, fluorene−thiophene oligomers substituted at both ends of the molecule by carbonyl groups are also investigated. It is shown that the optical properties of the polyesters are very close to those of the respective esters. On the other hand, the fluorescence quantum yield of the polyesters are smaller than those of the respective esters but their luminescence remains relatively intense. Molecular structures

* To whom correspondence should be addressed.
[†] Université de Montréal.
[‡] Université Laval.

10.1021/ma001042a CCC: $20.00
Published on Web 03/02/2001

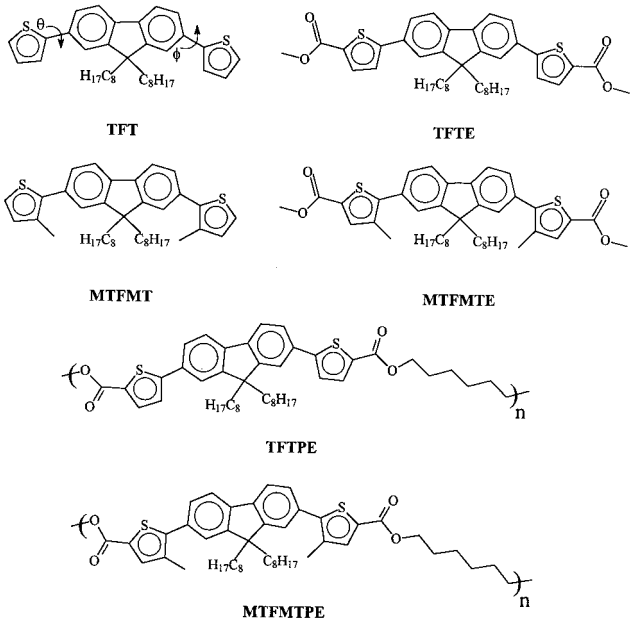

Figure 1. Molecular structure of the thiophene−fluorene−thiophene derivatives.

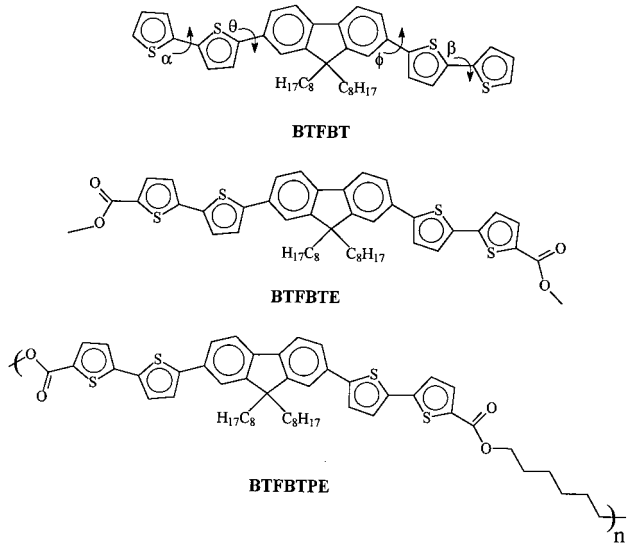

Figure 2. Molecular structure of the bithiophene−fluorene−bithiophene derivatives.

of the compounds investigated in this paper are displayed in Figures 1 and 2.

2. Experimental Section

2.1. Materials. Chloroform was purchased from A & C American Chemicals Ltd (spectrograde) and used as received. Prior to use, the solvent was checked for spurious emission in the region of interest and found to be satisfactory. Diisopropylamine (Aldrich) was dried and distilled over NaOH pellets. THF (Aldrich) was dried over sodium and benzophenone as drying indicator. Tetrakis (triphenylphosphine)palladium(0) was synthesized following the procedure reported in the literature.[31]

2.2. Synthesis and Characterization. 2,7-Bis(4,4,5,5-tetramethyl-1,3,2-dioxaborolan-2-yl)-9,9-dioctylfluorene (**1**), 5-bromo-2,2′-bithiophene (**2**), and 2-bromo-3-methylthiophene (**3**) were synthesized following the procedures reported in the literature.[24,32−35] 2-Bromothiophene (**4**) was obtained from Aldrich and used without purification.

5-Bromo-(2,2′-bithiophene)-5′-carboxylic acid (5). To a solution of 2.27 g of diisopropylamine (22.4 mmol, Aldrich) in anhydrous THF (2 mL) was added dropwise 8.16 mL (20.41 mmol) of *n*-butyllithium (2.5 M in hexaness, Aldrich), at −78 °C. The mixture was stirred at −78 °C for 20 min and at 0 °C for 20 min and cooled again at −78 °C. Compound **2** (5.0 g, 20.4 mmol) in anhydrous THF (200 mL) was added dropwise to the lithium diisopropylamine (LDA) solution and stirred for 30 min at −78 °C. Dry CO_2 (generated by warming dry ice and passing through drying tube) was added to the mixture. Dry CO_2 was bubbled for 30 min at −78 °C, followed by 2 h at room temperature. The mixture was poured into 50 mL of an aqueous 10% HCl solution. The organic layer was washed three times with water and dried over magnesium sulfate. The solvent was removed and the residue was purified by recrystallization in ethanol to provide 3.42 g (56%) of the title product as a yellow solid. Mp: 239−240 °C.

^{1}H NMR (300 MHz, DMSO-d_6), δ (ppm): 13.30 (s, 1H); 7.65 (d, 1H, J = 3.7 Hz); 7.31 (m, 2H); 7.25 (d, 1H, J = 3.7 Hz).

^{13}C NMR (75 MHz, DMSO-d_6), δ (ppm): 162.56; 141.44; 137.17; 134.18; 133.23; 131.88; 126.42; 125.08; 112.17.

HRMS: calculated for $C_9H_5BrO_2S_2$, 287.8914; found, 287.8910.

5-Bromo(methyl 2,2′-bithiophene-5′-carboxylate) (6). To a solution of 0.87 g of diisopropylamine (8.6 mmol, Aldrich) in anhydrous THF (2 mL) was added dropwise 3.26 mL (8.2 mmol) of *n*-butyllithium (2.5 M in hexaness, Aldrich), at −78 °C. The mixture was stirred at − 78 °C for 20 min, warmed to 0 °C for 20 min and cooled again at −78 °C. Compound **2** (2.0 g, 8.2 mmol) in anhydrous THF (80 mL) was added dropwise to the lithium diisopropylamine (LDA) solution and stirred for 30 min at −78 °C. Methyl chloroformate (1.26 mL, 16.3 mmol, Aldrich) was added to the mixture. The solution was warmed to room temperature and was kept under stirring for the night. The mixture was poured into water and extracted with diethyl ether. The organic extracts were washed with brine and dried over magnesium sulfate. The solvent was removed and the residue was purified by column chromatography (silica gel, 20% diethyl ether in hexanes) to provide 1.43 g (58%) of the title product as a red solid. Mp: 88−90 °C.

^{1}H NMR (300 MHz, CDCl3), δ (ppm): 7.67 (d, 1H, J = 4.4 Hz); 7.07 (d, 1H, J = 3.7 Hz); 7.02 (dd, 2H, J = 1.5 and 2.9 Hz); 3.89 (s, 3H).

^{13}C NMR (75 MHz, $CDCl_3$), δ (ppm): 162.36; 142.98; 137.77; 134.22; 131.80; 130.97; 125.33; 124.13; 113.00; 52.28.

HRMS: calculated for $C_{10}H_7BrO_2S_2$, 301.9071; found, 301.9073.

2-Bromo-3-methylthiophene-5-carboxylic Acid (7). To a solution of 4.20 g of diisopropylamine (41.5 mmol, Aldrich) in anhydrous THF (4 mL) was added dropwise 15.82 mL (39.5 mmol) of *n*-butyllithium (2.5 M in hexanes, Aldrich), at −78 °C. The mixture was stirred at −78 °C for 20 min, warmed to 0 °C for 20 min, and cooled again at −78 °C. Compound (**3**) (7.0 g, 39.5 mmol) in anhydrous THF (350 mL) was added dropwise to the lithium diisopropylamine (LDA) solution and stirred for 30 min at −78 °C. Dry CO_2 (generated by warming dry ice and passing through drying tube was introduced. Dry CO_2 was bubbled for 30 min at −78 °C, followed by 2 h at room temperature. The mixture was poured into 50 mL of an aqueous 1 M NaOH solution. The aqueous layer was washed three times with diethyl ether. The desired product was precipitated by neutralizing the water phase with 30% HCl and collect by filtration. The filtrate was washed several times with water and dried by vacuum to provide 6.21 g (71%) of the title product as a red-brown solid. Mp: 192−193 °C.

^{1}H NMR (300 MHz, $CDCl_3$), δ (ppm): 7.56 (s, 1H); 2.23 (s, 3H); 11.00 (s, 1H)

^{13}C NMR (75 MHz, $CDCl_3$),: δ (ppm): 162.20; 139.76; 135.94; 134.15; 117.30; 15.17.

HRMS: calculated for $C_6H_5BrO_2S$, 219.9194; found, 219.9198.

2-Bromo(methyl 3-methylthiophene-5-carboxylate) (8). Following the procedure used for the synthesis of compound **6**, a red solid was obtained after purification by column chromatography (silica gel, 7% ethyl acetate in hexanes). Mp: 34−35 °C. (Yield: 65%.)

^{1}H NMR (300 MHz, $CDCl_3$), δ (ppm): 7.45 (s, 1H); 3.84 (s, 3H); 2.18 (s, 3H).

^{13}C NMR (75 MHz, $CDCl_3$), δ (ppm): 161.40; 138.13; 134.55; 131.95; 117.34; 51.87; 14.87.

HRMS: calculated for $C_7H_7BrO_2S$, 233.9350; found, 233.9346.

2-Bromothiophene-5-carboxylic Acid (9). Following the procedure used for the synthesis of compound **7**, a yellow solid was obtained. Mp: 129−130 °C. (Yield: 72%.)

^{1}H NMR (300 MHz, $CDCl_3$), δ (ppm): 11.54 (s, 1H); 7.64 (d, 1H, J = 3.7 Hz); 7.11 (d, 1H, J = 4.4 Hz).

^{13}C NMR (75 MHz, $CDCl_3$), δ (ppm): 161.97; 136.50; 134.81; 132.38; 120.05.

HRMS: calculated for $C_5H_3BrO_2S$, 205.9037; found, 205.9041.

2-Bromo(methyl thiophene-5-carboxylate) (10). Following the procedure used for the synthesis of compound (**6**), a white solid was obtained after purification by column chromatography (silica gel, 20% diethyl ether in hexanes). Mp: = 53−55 °C (yield: 68%).

^{1}H NMR (300 MHz, $CDCl_3$), δ (ppm): 7.52 (d, 1H, J = 3.7 Hz); 7.04 (d, 2H, J = 4.4 Hz); 3.85 (s, 3H).

^{13}C NMR (75 MHz, $CDCl_3$), δ (ppm): 161.29; 134.47; 133.47; 130.70; 120.03; 52.08.

HRMS: calculated for $C_6H_5BrO_2S$, 219.9194; found, 219.9198.

Trimers. Trimers were obtained by using procedures to those reported by Beaupré et al.[36] Compound **1** (1 equiv), a monobrominated aromatic compound (3 equiv), and 0.5−1% M of $(PPh_3)_4Pd(0)$ were added to an aqueous mixture of THF/2 M K_2CO_3 (1.5/1). The mixture was poured into water and extracted with chloroform. The organic extracts were washed with brine and dried over magnesium sulfate.

2,7-Bis(2-thienyl)-9,9-dioctylfluorene (TFT) (11). Compounds **1** and **4** were used to give the title material as a green oil after purification by preparative plate (silica gel, 3% ethyl acetate in hexanes as eluent). (Yield: 67%.)

^{1}H NMR (300 MHz, $CDCl_3$), δ (ppm): 7.70 (m, 2H); 7.60 (m, 4H); 7.40 (dd, 2H, J = 0,7 and 2.6 Hz); 7.31(d, 2H, J = 4.8 Hz); 7.13 (m, 2H); 2.03 (m, 4H); 1.13 (m, 20 H); 0.81 (t, 6H, J = 6.6 Hz); 0.71 (m, 4H).

^{13}C NMR (75 MHz, $CDCl_3$), δ (ppm): 151.57; 145.03; 140.09; 133.17; 127.91; 124.86; 124.34; 122.76; 120.03; 119.97; 55.15; 40.27; 31.66; 29.86; 29.06; 29.03; 23.64; 22.45; 13.92

HRMS: calculated for $C_{37}H_{46}S_2$, 554.30408; found, 554.30290.

2,7-Bis(thien-2-yl-5-carboxylic acid)-9,9-dioctylfluorene (TFTA) (12). Compounds **1** and **9** were used to give the title material as a yellow solid after purification by column chromatography (silica gel, 10% ethyl acetate in hexanes as eluent). Mp: 263−264 °C. (Yield: 63%.)

^{1}H NMR (300 MHz, DMSO-d_6), δ (ppm): 7.90 (d, 2H, J = 7.7 Hz); 7.84 (s, 2H); 7.75 (m, 4H); 7.67 (d, 2H, J = 4.1 Hz); 2.06 (m, 4H); 1.00 (m, 20 H); 0.71 (t, 6H, J = 6.6 Hz); 0.52 (m, 4H).

^{13}C NMR (75 MHz, DMSO-d_6), δ (ppm): 162.79; 151.70; 150.37; 140.69; 134.36; 132.90; 132.12; 125.08; 124.50; 120.92; 120.16; 55.16; 31.14; 29.01; 28.42; 28.38; 23.23; 22.01; 13.81.

HRMS: calculated for $C_{39}H_{46}O_4S_2$, 642.2837; found, 642.2833.

2,7-Bis(methyl thien-2-yl-5-carboxylate)-9,9-dioctylfluorene (TFTE) (13). Compounds **1** and **10** were used to give the title material as a yellow solid after purification by column chromatography (silica gel, 10% ethyl acetate in hexanes as eluent). Mp: 93−95 °C. (Yield: 69%.)

^{1}H NMR (300 MHz, $CDCl_3$), δ (ppm): 7.80 (d, 2H, J = 4.1 Hz); 7.73 (d, 2H, J = 7.7 Hz); 7.64 (d, 2H, J = 8.1 Hz); 7.60 (m, 2H); 7.37 (d, 2H, J = 4.0 Hz); 3.93 (s, 6H); 2.01 (m, 4H); 1.12 (m, 20H); 0.78 (t, 6H, J = 7.0 Hz); 0.66 (m, 4H).

^{13}C NMR (75 MHz, $CDCl_3$), δ (ppm): 162.68; 152.09; 151.87; 141.17; 134.49; 132.63; 131.72; 125.40; 123.54; 120.58; 120.49; 55.49; 52.18; 40.27; 31.78; 29.91; 29.17; 29.14; 23.78; 22.60; 14.05.

HRMS: calculated for $C_{41}H_{50}O_4S_2$, 670.31506; found, 670.31270.

2,7-Bis(2,2′-bithien-5-yl)-9,9-dioctylfluorene (BTFBT) (14). Compounds **1** and **2** were used to give the title material as a yellow oil after purification by preparative plate (silica gel, 10% ethyl acetate in hexanes as eluent). (Yield: 27%.)

^{1}H NMR (300 MHz, $CDCl_3$), δ (ppm): 7.69 (d, 2H, J = 8.1 Hz); 7.62 (d, 2H, J = 1.5 Hz); 7.58 (d, 2H, J = 2.2 Hz); 7.31 (d, 2H, J = 4.4 Hz); 7.23 (s, 2H); 7.24 (d, 2H, J = 4.4 Hz); 7.20 (d, 2H, J = 4.4 Hz); 7.05 (dd, 2H, J = 4.4 and 1.5 Hz); 2.04 (m, 4H); 1.14 (m, 20H); 0.81 (t, 6H, J = 6.6 Hz); 0.71 (m, 4H).

^{13}C NMR (75 MHz, $CDCl_3$), δ (ppm): 151.28; 143.76; 140.19; 137.42; 136.33; 132.85; 127.75; 124.53; 124.21; 123.42; 123.27; 120.03; 119.70; 55.20; 40.25; 31.66; 29.84; 29.06; 29.03; 23.63; 22.46; 13.91.

HRMS calculated for $C_{45}H_{50}S_4$, 718.27720; found, 718.27277.

2,7-Bis(2,2′-bithien-5-yl-5′-carboxylic acid)-9,9-dioctylfluorene (BTFBTA) (15). Compounds **1** and **5** were used to give the title material as a yellow solid after purification by recrystallization in ethanol. Mp: 258−260 °C. (Yield: 72%.)

^{1}H NMR (300 MHz, DMSO-d_6), δ (ppm): 13.22 (s, 2H); 7.87 (d, 2H, J = 8.1 Hz); 7.79(s, 2H); 7.69 (m, 6H); 7.57 (d, 2H, J = 3.7 Hz); 7.43 (d, 2H, J = 3.7 Hz); 2.09 (m, 4H); 1.07 (m, 20 H); 0.72 (t, 6H, J = 6.6 Hz); 0.55 (m, 4H).

^{13}C NMR (75 MHz, DMSO-d_6), δ (ppm): 162.63; 151.55; 144.58; 142.79; 140.17; 134.43; 134.31; 132.57; 132.14; 127.05; 124.98; 124.58; 124.40; 120.71; 119.53; 55.07; 39.60; 39.04; 31.21; 29.07; 28.47; 23.27; 22.04; 13.84.

HRMS: calculated for $C_{45}H_{50}O_4S_4$, 718.2795; found, 718.2790.

2,7-Bis(methyl 2,2′-bithien-5-yl-5′carboxylate)-9,9-dioctylfluorene (BTFBTE) (16). Compounds **1** and **6** were used to give the title material as a yellow solid after purification by column chromatography (silica gel, 20% diethyl ether in hexanes as eluent). Mp: 129−131 °C. (Yield: 74%.)

^{1}H NMR (300 MHz, $CDCl_3$), δ (ppm): 7.70 (m, 4H); 7.60 (dd, 2H, J = 1.4 and 7.6 Hz); 7.55(m, 2H); 7.31 (dd, 4H, J = 3.7 and 7.7 Hz); 7.19 (d, 2H, J = 4.0 Hz); 2.03 (m, 4H); 1.13 (m, 20 H); 0.79 (t, 6H, J = 6.6 Hz); 0.69 (m, 4H).

^{13}C NMR (75 MHz, $CDCl_3$), δ (ppm): 162.48; 151.95; 145.73; 144.31; 135.25; 134.37; 132.71; 131.17; 126.24; 124.92; 123.90; 123.67; 120.41; 119.93; 55.42; 52.21; 40.35; 31.84; 29.98; 29.23; 29.20; 23.84; 22.64; 14.10.

HRMS: calculated for $C_{49}H_{54}O_4S_4$, 834.2905; found, 834.2925.

2,7-Bis(3-methylthien-2-yl)-9,9-dioctylfluorene (MTFMT) (17). Compounds **1** and **3** were used to give the title material as a green oil after purification by preparative plate (silica gel, 3% ethyl acetate in hexanes as eluent). (Yield: 36%.)

^{1}H NMR (300 MHz, $CDCl_3$), δ (ppm): 7.75 (d, 2H, J = 7.4 Hz); 7.48 (d, 2H, J = 1.5 Hz); 7.45 (s, 2H); 7.24 (d, 2H, J = 2.9 Hz); 6.98 (d, 2H, J = 5.2 Hz); 2.40 (s, 6H); 2.01 (m, 4H); 1.20 (m, 20H); 0.83 (t, 6H, J = 7.4 Hz); 0.77 (m, 4H).

^{13}C NMR (75 MHz, $CDCl_3$), δ (ppm): 151.08; 139.61; 138.47; 133.33; 132.87; 131.03; 127.75; 123.31; 122.98; 119.55; 55.03; 40.13; 31.58; 29.83; 29.03 (2C); 23.70; 22.41; 14.93; 13.88.

HRMS: calculated for $C_{39}H_{50}S_2$, 582.3354; found, 582.3357.

2,7-Bis(3-methylthien-2-yl-5-carboxylic acid)-9,9-dioctylfluorene (MTFMTA) (18). Compounds **1** and **7** were used to give the title material as a yellow solid after purification by recrystallization in ethanol. Mp: 218−220 °C. (Yield: 54%.)

^{1}H NMR (300 MHz, DMSO-d_6), δ (ppm): 13.05 (s, 1H); 7.93 (d, 2H, J = 8.1 Hz); 7.65 (s, 2H); 7.60 (s, 2H); 7.50 (dd, 2H, J = 8.1 and 1.5); 2.53 (m, 4H); 1.07 (m, 20H); 0.74 (t, 6H, J = 6.6 Hz); 0.58 (m, 4H).

^{13}C NMR (75 MHz, DMSO-d_6), δ (ppm): 162.86; 151.10; 144.55; 136.84; 134.01; 132.35; 131.48; 127.69; 123.05; 120.52; 54.99; 31.12; 29.10; 28.47; 28.44; 23.35; 22.01; 14.80; 13.78.

HRMS: calculated for $C_{41}H_{50}O_4S_2$, 670.3150; found, 670.3162.

2,7-Bis(methyl 3-methylthien-2-yl-5-carboxylate)-9,9-dioctylfluorene (MTFMTE) (19). Compounds **1** and **8** were used to give the title material as a brown oil after purification by column chromatography (silica gel, 10% ethyl acetate in hexanes as eluent). (Yield: 68%.)

^{1}H NMR (300 MHz, $CDCl_3$), δ (ppm): 7.76 (d, 2H, J = 7.7 Hz); 7.67 (s, 2H); 7.47 (d, 4H, J = 10.3); 3.91 (s, 6H); 2.37 (s, 6H); 2.00 (m, 4H); 1.14 (m, 20H); 0.80 (t, 6H, J = 6.6 Hz); 0.70 (m, 4H).

^{13}C NMR (75 MHz, $CDCl_3$), δ (ppm): 162.82; 151.58; 146.17; 140.51; 137.26; 134.03; 132.77; 130.07; 127.99; 123.47; 120.14; 52.13; 40.21; 31.75; 30.01; 29.94; 29.19; 29.16; 23.87; 22.60; 15.22; 14.05.

HRMS: calculated for $C_{43}H_{54}O_4S_2$, 698.3464; found, 698.3477.

2,7-Bis(thien-2-yl-5-carbonyl chloride)-9,9-dioctylfluorene (TFTAC) (20). To a solution of 0.6 g of compound **12**

(0.9 mmol) in benzene (5 mL) to reflux was added dropwise 2.05 mL (28.0 mmol) of thionyl chloride (Aldrich). The mixture was stirred to reflux for 24 h. The excess of thionyl chloride and benzene was distilled and the crude product was purified by recrystallization in hexanes. Mp: 112−113 °C. (Yield: 81%.)

^{1}H NMR (300 MHz, $CDCl_3$), δ (ppm): 7.98 (d, 2H, J = 3.7 Hz); 7.78 (d, 2H, J = 8.1 Hz); 7.69 (d, 2H, J = 8.1 Hz); 7.63 (s, 2H); 7.46 (d, 2H, J = 3.7 Hz); 2.05 (m, 4H); 1.15 (m, 20H); 0.78 (t, 6H, J = 6.6 Hz); 0.66 (m, 4H).

^{13}C NMR (75 MHz, $CDCl_3$), δ (ppm): 159.35; 157.33; 152.43; 141.97; 139.07; 134.96; 132.10; 125.81; 124.43; 121.00; 120.73; 55.71; 40.20; 31.77; 29.86; 29.16 (2C); 23.80; 22.62; 14.06.

HRMS: calculated for $C_{39}H_{44}Cl_2O_2S_2$, 678.2160; found, 678.2164.

2,7-Bis(2,2′-bithien-5-yl-5′-carbonyl chloride)-9,9-dioctylfluorene (BTFBTAC) (21). Following the procedure used for the synthesis of compound **20** (using compound **15**), an orange oil was obtained after purification by flash chromatography (silica gel, in chloroform). (Yield: 47%.)

^{1}H NMR (300 MHz, $CDCl_3$), δ (ppm): 7.90 (d, 2H, J = 4.4 Hz); 7.72 (d, 2H, J = 8.1 Hz); 7.62 (d, 2H, J = 6.6 Hz); 7.56 (s, 2H); 7.39 (d, 2H, J = 3.7 Hz); 7.37 (d, 2H, J = 3.7 Hz); 7.25 (d, 2H, J = 3,0 Hz); 2.04 (m, 4H); 1.16 (m, 20H); 0.79 (t, 6H, J = 3.7 Hz); 0.69 (m, 4H).

^{13}C NMR (75 MHz, $CDCl_3$), δ (ppm): 158.87; 151.89; 149.58; 147.29; 140.73; 138.89; 136.93; 134.02; 132.28; 127.45; 124.90; 124.08; 123.94; 120.36; 119.90; 55.30; 40.13; 34.96; 31.64; 29.77; 29.02; 23.63; 22.44; 13.91.

HRMS: calculated for $C_{47}H_{48}Cl_2O_2S_4$, 842.1914; found, 842.1933.

2,7-Bis(3-methylthien-2-yl-5-carbonyl chloride)-9,9-dioctylfluorene (MTFMTAC) (22). Following the procedure used for the synthesis of compound **20** (using compound **18**), a green oil was obtained after purification by flash chromatography (silica gel, in chloroform). (Yield: 41%.)

^{1}H NMR (300 MHz, $CDCl_3$), δ (ppm): 7.82 (m, 4H); 7.48 (m, 4H); 2.40 (s, 6H); 2.02 (m, 4H); 1.17 (m, 20H); 0.80 (t, 6H, J = 6.6 Hz); 0.70 (m, 4H).

^{13}C NMR (75 MHz, $CDCl_3$), δ (ppm): 159.38; 152.18; 151.90; 141.44; 135.32; 132.19; 128.10; 123.51; 123.42; 120.58; 55.61; 40.14; 31.77; 29.89; 29.19; 29.16; 23.90; 22.62; 15.29; 14.08.

HRMS: calculated for $C_{41}H_{48}Cl_2O_2S_2$, 706.2473; found, 706.2484.

Poly(1,6-hexane-2,7-bis(thien-2-yl-5-dicarboxylate)-9,9-dioctylfluorene) (TFTPE) (23). In a 5 mL flask were mixed 0.3241 g (0.46 mmol) of compound **20** and 0.0562 g (0.46 mmol) of 1,6-hexanesdiol (Aldrich) under nitrogen at 125 °C for 4 h. The temperature was raised to 160 °C and the flask was put under reduced pressure to evacuate HCl formed during the condensation reaction. The crude product was precipitated in methanol at 0 °C, washed with acetone, and then dried under reduced pressure for 24 h. (Yield: 24%.)

^{1}H NMR (300 MHz, $CDCl_3$), δ (ppm): 7.71 (d, 2H, J = 4.4 Hz); 7.63 (d, 2H, J = 8.1 Hz); 7.55 (m, 4H); 7.28 (d, 2H, J = 3.7 Hz); 4.28 (t, 4H, J = 6.6 Hz); 1.95 (m, 4H); 1.75 (m, 4H); 1.48 (m, 4H); 1.07 (m, 20H); 0.70 (t, 6H, J = 6.6 Hz); 0.60 (m, 4H).

M_n: 12000. M_w: 44000.

Poly(1,6-hexane-2,7-bis(2,2′-bithien-5-yl-5′-dicarboxylate)-9,9-dioctylfluorene) (BTFBTPE) (24). The same procedure used for the synthesis of compound **23** has been followed (using monomer **21**). (Yield: 21%.)

^{1}H NMR (300 MHz, $CDCl_3$), δ (ppm): 7.71 (m, 4H); 7.55 (m, 4H); 7.28 (m, 4H); 7.17 (d, 2H, J = 2.9 Hz); 4.32 (m, 4H); 2.03 (m, 4H); 1.81 (m, 4H); 1.54 (m, 4H); 1.06 (m, 20 H); 0.87 (m, 6H); 0.77 (m, 4H).

M_n: 6000. M_w: 13000.

Poly(1,6-hexane-2,7-bis(3-methylthien-2-yl-5-dicarboxylate)-9,9-dioctylfluorene) (MTFMTPE) (25). The same procedure used for the synthesis of compound **23** has been followed (using monomer **22**). (Yield: 23%.)

^{1}H NMR (300 MHz, $CDCl_3$), δ (ppm): 7.67 (d, 2H, J = 7.4 Hz); 7.58 (s, 2H); 7.39 (m, 4H); 4.25 (t, 4H, J = 6.6 Hz); 2.29 (s, 6H); 1.93 (m, 4H); 1.72 (m, 4H); 1.46 (m, 4H); 1.09 (m, 20H); 0.72 (t, 6H, J = 6.6 Hz); 0.62 (m, 4H).

M_n: 8000. M_w: 14000.

2.3. Instrumentation. Number-average (M_n) and weight-average (M_w) molecular weights were determined by size exclusion chromatography (SEC) with HPLC pump using a Waters UV−visible detector. The calibration curve was made with a series of monodispersed polystyrene standards in tetrahydrofuran (HPLC grade, Aldrich). Absorption spectra were recorded on a Varian Cary 1 Bio UV/vis spectrophotometer at room temperature using 1 cm quartz cells and solute concentrations of (1−3) × 10^{-5} M. It has been verified that the Beer−Lambert law is well-respected in the region of the concentrations used. Fluorescence spectra corrected for the emission detection were recorded on a Spex Fluorolog-2 spectrophotometer with a F2T11 special configuration. Excitation and emission band-passes used were 2.6 and 1.9 nm, respectively. Each solution was excited near the absorption wavelength maximum using a 1 cm path length quartz cell. Solution concentrations used were (1−3) × 10^{-6} M, giving absorbances always less than 0.1 to avoid any inner-filter effects. For all molecules, a study of the concentration (C) effect has been done on the fluorescence intensity (I_F), and all measurements have been performed in the linear region of the I_F vs C curve. All corrected fluorescence excitation spectra were found to be equivalent to their respective absorption spectra. Quantum yields of fluorescence were determined in argon-saturated solutions of the substrates at 298 K against anthracene in ethanol (ϕ_f = 0.27) as a standard.[37]

Fluorescence lifetimes were measured on a multiplexed time-correlated single photon counting fluorimeter (Edinburgh Instruments, model 299T) at 298 K. Details on the instrument have been published elsewhere.[38] The instrument incorporates an all-metal coaxial hydrogen flashlamp. Reconvolution analysis was performed by fitting over all the fluorescence decay including the rising edge. The kinetic interpretation of the goodness-of-fit was assessed using plots of weighted residuals, reduced χ^2 values, and Durbin−Watson (DW) parameters.

2.4. Calculation methodology. Ab initio calculations were performed on a Pentium III (450 Mz) personal computer with 128 Mb RAM using the Gaussian 98W program, version 5.2.[39] The geometries were optimized at the HF level with the 6-31G* basis set. The Berny analytical gradient method was used for the optimizations. The requested HF convergence on the density matrix was 10^{-8}, and the threshold values for the maximum force and the maximum displacement were 0.00045 and 0.0018 au, respectively.

The ZINDO/S method including configuration interaction (CI) as employed in the HYPERCHEM package (version 5.01) was used to calculate the singlet−singlet electronic transition energies of the optimized conformers. ZINDO/S is a modified INDO method parametrized to reproduce UV/visible spectroscopic transitions.[40,41] The electron-repulsion integrals were evaluated using the Mataga−Nishimoto formula. All singly excited configurations involving the 20 highest occupied and the 20 lowest unoccupied orbitals (CI = 20/20) were included in the energy calculation.

3. Results and Discussion

3.1. Optical Properties. The absorption and fluorescence spectra of the thiophene−fluorene co-oligomers as well as their corresponding polyesters have been recorded in chloroform at room temperature and are shown in Figures 3−5. Their spectral data are reported in Table 1.

The first absorption band of TFT is centered at 354 nm and does not show any resolvable vibronic fine structure suggesting that this molecule is relatively flexible in its ground state. In contrast, the fluorescence spectrum of TFT shows four vibronic peaks, indicating that the molecule is more rigid in its first relaxed excited state. In agreement with this statement, one can see that the fluorescence spectrum of TFT is much sharper than its absorption band suggesting the existence of a

Table 1. Spectroscopic Parameters of Thiophene−Fluorene Co-oligomers and Their Corresponding Polyesters in Chloroform at Room Temperature (298 K)

molecule	λ_A[a] (nm)	ν_A[b] (cm^{-1})	ϵ[c] (M^{-1} cm^{-1})	$fwhm_A$[d] (cm^{-1})	λ_F[e] (nm)	ν_F[f] (cm^{-1})	$fwhm_F$[g] (cm^{-1})
TFT	354	28 200	49 600	4200	386	25 900	2600
TFTE	378	26 500	66 100	3700	419	23 900	2900
TFTPE	379	26 400		4300	421	23 800	3900
MTFMT	337	29 700	43 900	4800	386	25 900	3100
MTFMTE	354	28 200	54 100	4500	419	23 900	3100
MTFMTPE	356	28 100		4700	423	23 600	3900
BTFBT	399	25 100	82 000	4200	445	22 500	2500
BTFBTE	418	23 900	109 000	4300	472	21 200	2900
BTFBTPE	414	24 200		4900	479	20 900	3800

[a] Absorption wavelengths taken at the maximum of the absorption band. [b] Absorption wavenumbers taken at the maximum of the absorption band. [c] Absorption coefficient at the maximum of the absorption band. [d] Full width at half-maximum (fwhm) of the absorption band. [e] Fluorescence wavelengths at the maximum of the first vibronic fluorescence peak (0−0 band). [f] Fluorescence wavenumbers at the maximum of the first vibronic fluorescence peak (0−0 band). [g] Full width at half-maximum (fwhm) of the fluorescence band.

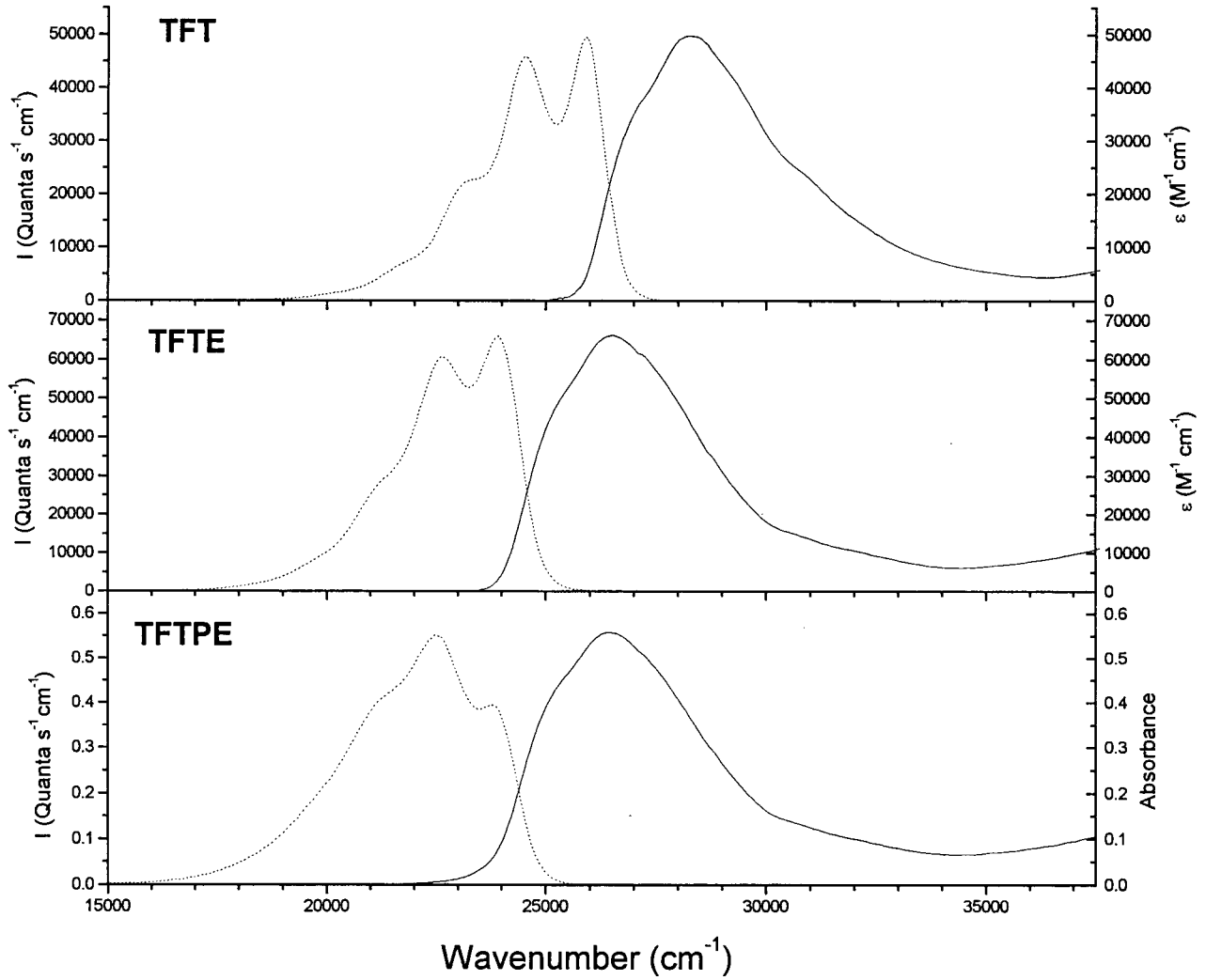

Figure 3. Absorption (−) and fluorescence (···) spectra of TFT and TFTE as well as their corresponding polyester (TFTPE) in chloroform. The fluorescence intensities have been normalized relative to the first absorption band of each compound.

narrower distribution of conformers in the excited state (see Figure 3 and Table 1).

The addition of carbonyl groups at both ends of TFT provokes a large red-shift of the absorption and fluorescence bands in TFTE. Two effects might be responsible for this behavior: (1) an increase in the conjugation length due to the addition of two double bonds to the molecular frame and (2) a decrease in the twisting between thiophene and fluorene rings caused by inductive effects of the substituents. To distinguish between these two effects, HF/6-31G* ab initio calculations have been performed on both molecules. To reduce the time scale of the calculations, the octyl chains at the 9-position of the fluorene ring have been replaced by ethyl groups. We have shown recently that the presence of alkyl chains in the 9-position does not significantly affect the equilibrium geometry of fluorene derivatives.[30] The dihedral angles between adjacent rings are summarized in Table 2. One can see that torsional angles of TFT and TFTE are very similar, ruling out effect 2 above. One can then conclude that an increase in the conjugation length is solely responsible for the spectral

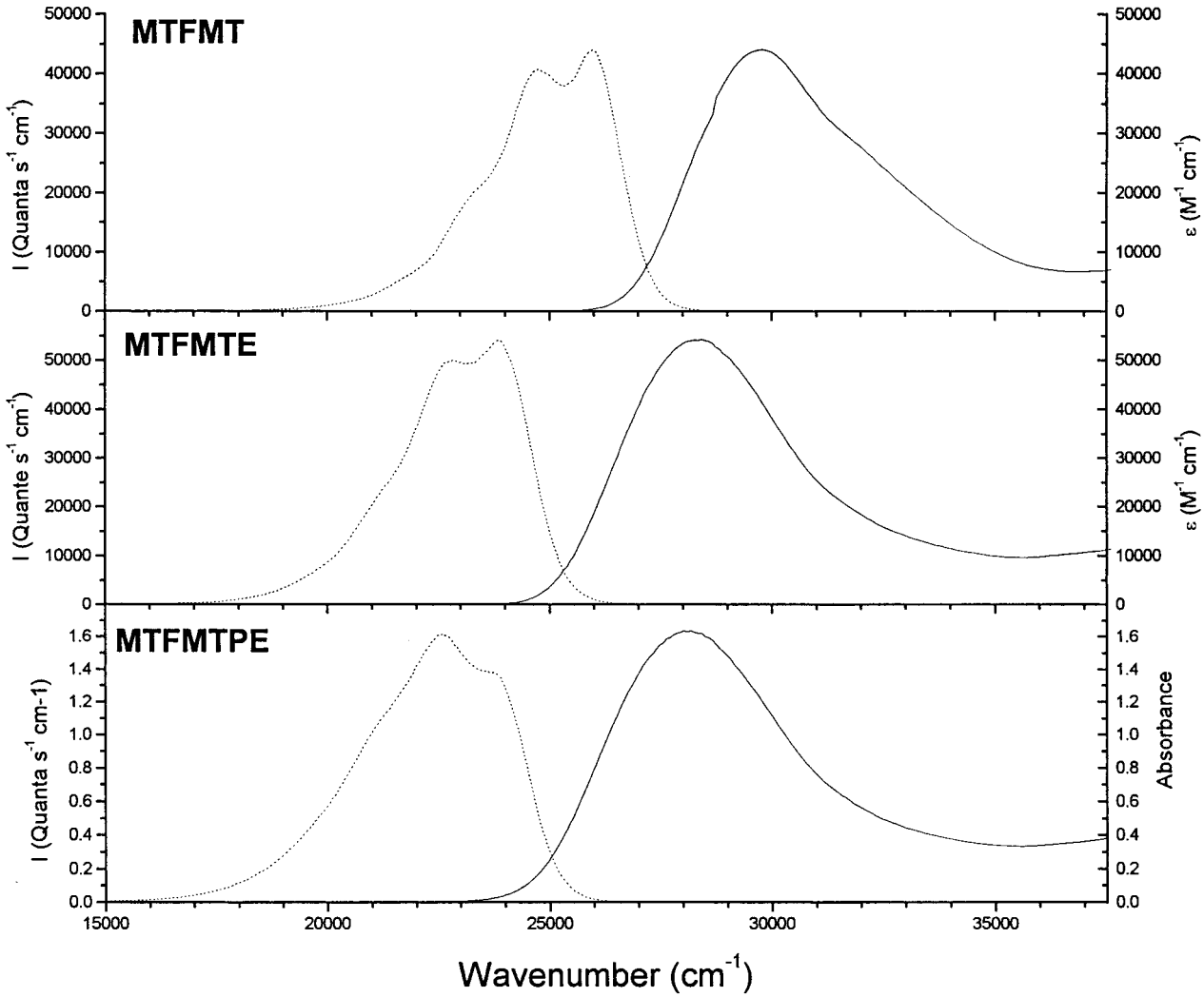

Figure 4. Absorption (−) and fluorescence (···) spectra of MTFMT and MTFMTE as well as their corresponding polyester (MTFMTPE) in chloroform. The fluorescence intensities have been normalized relative to the first absorption band of each compound.

Table 2. Dihedral Angles of Thiophene−Fluorene Co-oligomers As Obtained by HF/6-31G* ab Initio Calculations

molecule	α (deg)	θ (deg)	φ (deg)	β (deg)
TFT		141.0	141.0	
TFTE		141.6	141.6	
MTFMT		125.4	125.4	
MTFMTE		126.9	126.9	
BTFBT	149.0	141.8	141.8	149.0
BTFBTE	152.0	141.7	141.7	152.0

shifts observed in TFTE without any important conformational changes.

Table 1 and Figure 3 show that the absorption and fluorescence band maxima of TFTPE are very close to those obtained for TFTE. It thus seems that the thiophene−fluorene−thiophene units are well isolated in the polyester chain. However, judging by the bandwidths of these spectra, a wider distribution of conformers seems to exist for the chromophore incorporated in the polyester in its ground and excited states.

The addition of methyl groups in the 3-position of each thiophene ring to form the MTFMT molecule induces an important blue shift of the band (17 nm) compared to TFT whereas its absorption coefficient is reduced. This shows that the steric hindrance between the methyl groups and the phenyl rings creates a twisting between thiophene and phenyl rings causing a reduction in the electronic conjugation along the molecular frame. This is confirmed by HF/6-31G* ab initio calculations. Indeed, Table 2 shows that MTFMT is more twisted than TFT. Moreover, the absorption band of MTFMT is much wider than that of TFT confirming the existence of a wider conformer distribution for MTFMT in its ground state. In other words, the MTFMT torsional potential surface should be flatter near the global minimum compared to that of TFT as reported recently for 2-(3,4-dimethylthiophene)-2′-fluorene vs 2-thiophene-2′-fluorene.[42]

In contrast to the absorption data, the fluorescence spectra of TFT and MTFMT appear at the same energy. It thus seems that, in the relaxed S_1 excited state, electronic delocalization is favored in such a way that the steric hindrance causes by the alkyl chains is much reduced. Such a behavior has also been observed recently for fluorene−thiophene dyads.[30] Moreover, the fluorescence spectra of both molecules are structured and are sharper than their respective absorption spectra (see Figures 3 and 4). This indicates that the fluorene−thiophene rotational energy barriers are much larger in the excited-state such that a narrower distribution of conformers, characterized by more rigid planar conformations of the molecules, should exist.

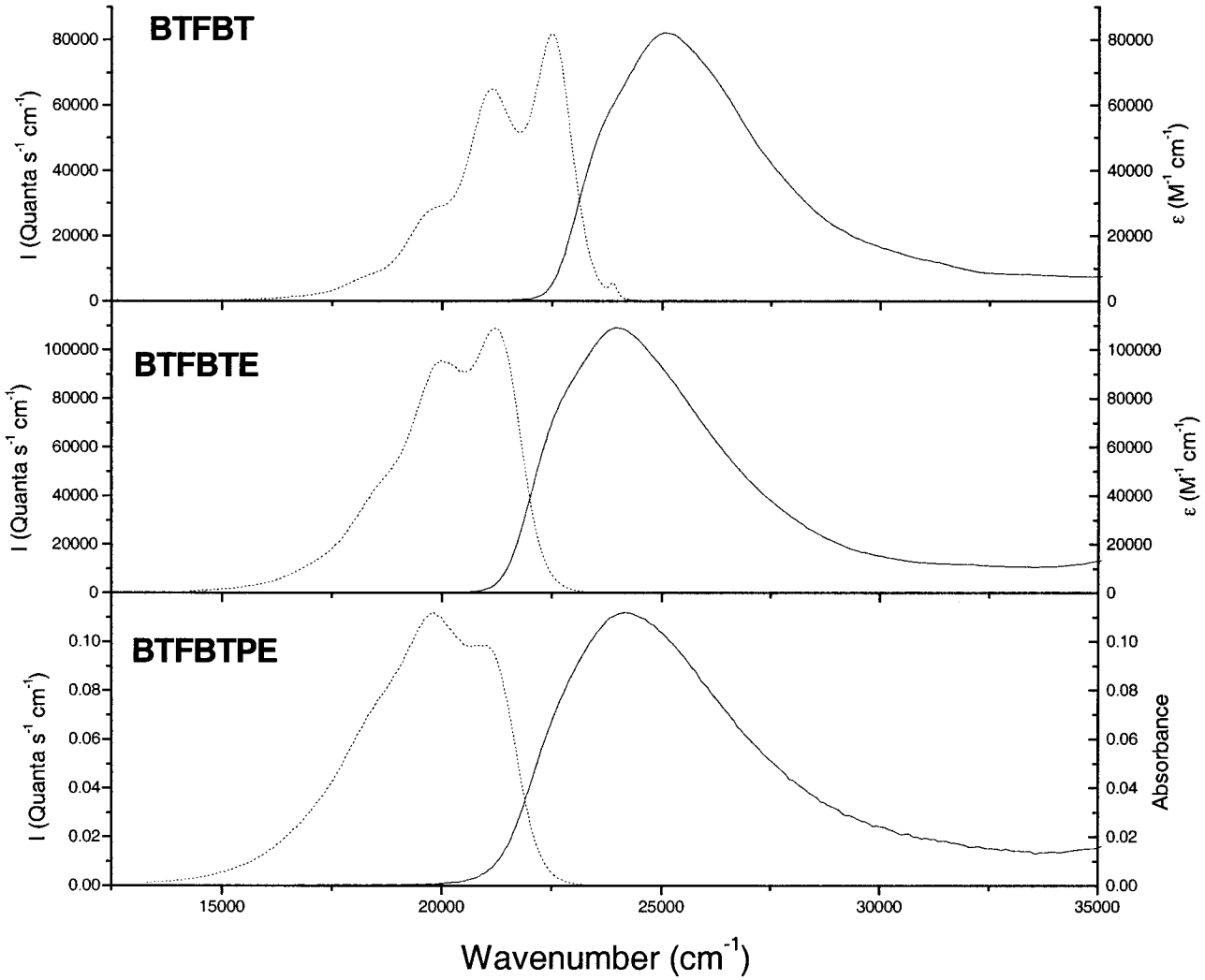

Figure 5. Absorption (−) and fluorescence (···) spectra of BTFBT and BTFBTE as well as their corresponding polyester (BTFBTPE) in chloroform. The fluorescence intensities have been normalized relative to the first absorption band of each compound.

The effect of adding ester groups on the spectral properties of MTFMT is the same as that observed for TFT. Both absorption and fluorescence bands are red-shifted showing a better electronic conjugation which should improve the molecular rigidity in the ground and excited states (see Figure 4 and Table 1). According to HF/6-31G* ab initio calculations reported in Table 2, we believe that the molecular conformation of MTFMTE should be similar to that of MTFMT.

Judging by the spectral positions of MTFMT and MTFMTPE, the triad units seem well isolated in the polyester chain. However, as observed above for TFTPE, the absorption and fluorescence bandwidths of the polyester are larger than that of MTFMTE. This suggests that the incorporation of the triad unit in the polyester chain increases the number of conformers present in the polymer.

Compared to the absorption and fluorescence spectra of TFT, the optical transitions of BTFBT are red shifted due to the increase of the conjugation length (see Figure 5 and Table 1). Moreover one can see in Table 2 that the torsional angles between thiophene and fluorene rings of both molecules are very close. This clearly indicates that increasing the conjugation length does not improve the molecular planarity of thiophene−fluorene oligomers. Accordingly, the absorption and fluorescence bandwidths of TFT and BTFBT are very similar.

As shown above for TFT and MTFMT, the addition of ester groups to BTFBT induces a red shift in the absorption and fluorescence spectra of BTFBTE. Moreover, Table 2 shows that this substitutional effect does not significantly affect the dihedral angles between fluorene and thiophene rings. However HF/6-31G* ab initio calculations indicate that the bithiophene units are slightly more planar in the case of BTFBTE. It is worth pointing out that the observed red shift is less than that observed for the TFT/TFTE couple. The reason for this behavior might be explained by the fact that the initial electronic conjugation is longer for BTFBT compared to that of TFT, thus diminishing the effect of the ester groups at both ends of the molecule.

Finally, judging by the spectral positions of BTFBT and BTFBTPE, no interaction between oligomer units seems to exist in the polyester chain. But, as observed for TFTPE and MTFMTPE, the distribution of conformers seems to be affected when the oligomers are incorporated in a polyester chain.

3.2. Electronic Excitations. The nature and the energy of the HOMO and LUMO of these thiophene−fluorene co-oligomers, which are mainly involved in the first singlet−singlet electronic excitation (see below),

Table 3. HOMO, LUMO, and HOMO−LUMO Energy Gap of Thiophene−Fluorene Co-oligomers as Obtained from HF/6-31G* ab Initio Calculations

molecule	HOMO (eV)	LUMO (eV)	HOMO−LUMO (eV)
TFT	−7.240	2.089	9.33
TFTE	−7.532	1.519	9.05
MTFMT	−7.386	2.315	9.70
MTFMTE	−7.638	1.816	9.45
BTFBT	−7.109	1.803	8.91
BTFBTE	−7.261	1.503	8.76

have been investigated at the HF/6-31G* level. Both molecular orbitals of each derivative are delocalized along the long molecular axis and involve mainly p_z (out of plane axis) atomic orbitals (figure not shown). The nature of the molecular orbitals remains unchanged along the oligomers investigated. As observed recently for fluorene−thiophene dyads, the HOMO of each derivative possesses an antibonding character between fluorene and thiophene rings, which may explain the nonplanarity observed for these derivatives in their ground electronic state.[30] On the other hand, the LUMO of all the derivatives shows a bonding character between adjacent rings. This implies that the promotion of an electron from the HOMO to the LUMO is indeed improving the molecular planarity of these derivatives as suggested above from the fluorescence spectra.

The energies of the HOMO and LUMO are given in Table 3. One can see that both HOMO and LUMO of the ester derivatives are stabilized compared to the corresponding molecules without carbonyl groups. However, the LUMO is more stabilized than the HOMO by the addition of ester groups to the molecular frame. Consequently, the HOMO−LUMO energy gaps are smaller for the ester derivatives (see Table 3). On the other hand, the addition of a methyl group in the 3-position of the thiophene rings slightly stabilized the HOMO and destabilized the LUMO orbitals. The overall result is an increase in the HOMO−LUMO energy gaps for the methylated derivatives. This is well explained by the nature of the molecular orbitals. Indeed, the presence of the methyl groups induces a torsion in the molecule which should reduce the electronic conjugation over the whole molecule (see above). Thus, the HOMO which shows inter-ring antibonding character are stabilized whereas the LUMO is destabilized due to the strong bonding character involved between adjacent rings.

The reverse is true for the molecular orbitals of BTFBT compared to that of TFT. Indeed, the increase in the conjugation length destabilized the HOMO of BTFBT compared to that of TFT showing the antibonding character of the HOMO in these oligomers. On the other hand, the LUMO of BTFBT is stabilized compared to that of TFT in agreement with the bonding character of the LUMOs of both molecules.

The ZINDO/S semiempirical method has been used to obtain the nature and the energy of the first 10 singlet−singlet electronic transitions in the oligomers. The $\pi\pi^*$ overlap weighting factor has been ajusted to 1.548 in order to reproduce the S_1 origin of fluorene (33779 cm^{-1}) measured in a supersonic jet.[43] Optimized geometries (HF/6-31G*) have been used in the calculations. All electronic transitions are of the $\pi\pi^*$ type and involve both fluorene and thiophene rings. In other words, no localized electronic transitions on one particular ring are calculated among the first 10 singlet−singlet transitions. Excitation to the S_1 state corresponds mainly to the promotion of an electron from the HOMO to the LUMO. The oscillator strength (f) and the transition dipole moment along the long axis of the molecule (x) of the $S_1 \leftarrow S_0$ electronic transition are large, indicating that this transition is strongly allowed. The $S_1 \leftarrow S_0$ electronic excitation properties are summarized in Table 4. It is observed that the excitation energies of the first electronic transition follow the relative values of the HOMO−LUMO energy gaps computed in Table 3. However, the first electronic transition is much lower in energy compared to the computed HOMO−LUMO gap because of the configuration interaction (CI = 20/20) employed in the ZINDO/S calculations and also due to the fact that no scaling energy gap was used in Table 3.[44]

Table 4. First Singlet−Singlet Electronic Transition Data Obtained by the ZINDO/S Semiempirical Method for the Thiophene−Fluorene Co-oligomers at the HF/6-31G* Optimized Geometry

molecule	energy (cm^{-1})	f	transition dipole moment (D)		
			X^a	Y	Z
TFT	30 030	1.37	9.83	0.55	0.034
TFTE	28 345	1.81	11.6	0.73	0.16
MTFMT	31 104	1.06	8.53	0.22	0.13
MTFMTE	29 360	1.49	−10.4	−0.51	0.19
BTFBT	27 352	2.26	−13.2	−0.067	0.77
BTFBTE	26 205	2.19	−13.3	0.26	−0.38

[a] X is the long molecular axis.

The $S_1 \leftarrow S_0$ excitation energy of TFT is computed at 30030 cm^{-1} and should correspond to the first absorption band of this molecule measured at 28 200 cm^{-1} and having a large absorption coefficient (49 600 M^{-1} cm^{-1}). An energy decrease of 1685 cm^{-1} is computed for the S_1 state of TFTE compared to that of TFT. This is in very good agreement with the red shift observed for the absorption band of TFTE compared to that of TFT (1700 cm^{-1}, see Table 1). Moreover one can see in Table 4 that the oscillator strength (f) of the $S_1 \leftarrow S_0$ transition of TFTE is higher than that of TFT in agreement with the increase in the conjugation length for TFTE suggested in the previous section. A similar correlation has been found for the absorption coefficients of both molecules (see Table 1).

The $S_1 \leftarrow S_0$ electronic transition of MTFMT is compiled at 31 104 cm^{-1}, which is higher in energy by 1074 cm^{-1} compared to that of TFT. A similar blue shift has been observed experimentally for the absorption band of MTFMT compared to that of TFT (1500 cm^{-1}, see Table 1). The reason for this behavior involves a decrease in the electronic conjugation along the long molecular axis caused by the steric effects induced by the presence of the methyl groups. Similar results have been observed recently for the first absorption band of 2-(9,9-dioctylfluorene-2-yl)thiophene vs 2-(9,9-dioctylfluoren-2-yl)3-methylthiophene.[30] As a consequence of the steric effects, f and ϵ values for the first singlet−singlet transition of MTFMT are smaller than that of TFT.

The first electronic transition of MTFMTE is redshifted by 1744 cm^{-1} compared to that of MTFMT. These results are in fair agreement with the optical properties of both molecules, where a red shift of 1500 cm^{-1} is observed for the first absorption band of TFTME compared to that of MTFMT (see Table 1). Moreover, Table 1 also shows that the absorption coefficient for the $S_1 \leftarrow S_0$ electronic transition of MTFMTE is larger

Table 5. Photophysical Properties of Thiophene−Fluorene Co-oligomers as well as Their Corresponding Polyesters in Chloroform at Room Temperature (298 K)

molecule	ϕ_F	τ_F (ns)	$10^{-8}k_F$[a] (s^{-1})	$10^{-8}k_{nr}$[b] (s^{-1})
TFT	0.75	0.96	7.8	2.6
TFTE	0.67	1.00	6.7	3.3
TFTPE	0.46	0.80	5.8	6.8
MTFMT	0.64	0.59	10.8	6.1
MTFMTE	0.47	0.81	5.8	6.5
MTFMTPE	0.36	0.56	6.4	11.4
BTFBT	0.45	0.59	7.6	9.3
BTFBTE	0.36	0.71	5.1	9.0
BTFBTPE	0.20	0.42	4.8	19.0

[a] $k_F = \phi_F/\tau_F$ (radiative fluorescence decay rate constant). [b] $k_{nr} = k_F(1 - \phi_F)/\phi_F$ (nonradiative fluorescence decay rate constant).

than that of MTFMT in agreement with the computed *f* values of both molecules (see Table 4).

The first electronic transition of BTFBT is computed at 27 352 cm^{-1} and should correspond to the absorption band measured at 25 100 cm^{-1}. Compared to TFT, a red-shift of 2678 cm^{-1} is calculated for the $S_1 \leftarrow S_0$ transition of BTFBT. This is in fair agreement with experimental results, where a red-shift of 3100 cm^{-1} has been measured for the first absorption band of BTFBT compared to that of TFT. Finally, the addition of carbonyl groups to BTFBT induces a red-shift for the first electronic transition of BTFBTE, but to a lesser extent than that computed for TFTE (see Table 4). A similar behavior has been observed experimentally (see Table 1).

3.3. Molecular Photophysics. The fluorescence quantum yields (ϕ_F) and lifetimes (τ_F) as well as the radiative ($k_F = \phi_F/\tau_F$) and nonradiative ($k_{nr} = k_F(1 - \phi_F)/\phi_F$)) decay rate constants of all the compounds are reported in Table 5. For all fluorescence decay profiles, a single-exponential fit gives acceptable statistics parameters ($\chi^2 < 1.3$ and DW ≈ 1.7).

Table 5 shows that ϕ_F and particularly τ_F of MTFMT are smaller than those of TFT, giving rise to a higher value of k_{nr}. Judging by the fluorescence bandwidth of MTFMT, which is larger than that of TFT, more conformers seem present in the MTFMT relaxed S_1 excited state. Thus, for MTFMT, the increase in k_{nr} may involve an increase in the molecular flexibility. It is also worth noting that the fluorescence quantum yield of MTFMT remains high because its radiative decay constant is larger than that of TFT. The inductive effects of the methyl groups may be responsible for this behavior.

One can see in Table 5 that a higher value of k_{nr} is observed for BTFBT compared to that of TFT while the k_F values of both molecules are very close. For oligothiophenes, it is well established that the main deactivation pathway of the S_1 state involves an intersystem crossing process due to the presence of heavy sulfur atoms.[45,46] Accordingly, the intersystem crossing probability of BTFBT, which possesses two additional sulfur atoms, should increase and contribute to reduce the luminescence intensity.

It is also shown in Table 5 that ester derivatives possess fluorescence quantum yields which are smaller than those of the corresponding unsubstituted molecules. A decrease of the k_F values of the ester derivatives is mainly responsible for this behavior. This suggests that the ester derivatives would be more twisted in the relaxed S_1 state compared to the molecules without carbonyl groups. Along these lines, it is observed that the fluorescence bandwidths of TFTE and BTFBTE are larger than that of TFT and BTFBT. This shows that relaxed excited states do not necessarily behave like ground states or Franck−Condon excited states.

Finally, the fluorescence quantum yield and lifetime of the polyesters are reduced compared to that of the ester derivatives (see Table 5). An increase in the nonradiative decay constant is mainly responsible for this behavior. According to the fluorescence spectra reported above, the emission bandwidths of the polyesters are much larger than that of the isolated esters. Thus, we believe that the adjacent rings of the TFT units are more flexible when incorporated in a polyester chain, which should contribute to increase the nonradiative decay constant. However the emission of the polymers remains quite intense. Preliminary photoluminesncence measurements in the solid state have revealed a slight red shift of the emission spectrum when compared to the solution measurements but with no excimer formation. All these results indicate that these polyesters represent interesting materials for LED applications which, as shown with previous photoluminescent polyesters,[47] could even lead to polarized emission.

4. Concluding Remarks

The first absorption band of each derivative can be assigned to the calculated $S_1 \leftarrow S_0$ electronic transition. Excitation to the S_1 state corresponds mainly to the promotion of an electron from the HOMO to the LUMO. The HOMO possesses an antibonding character between neighboring rings which should contribute to the nonplanarity observed for these derivatives in their ground states. On the other hand, the LUMO shows bonding character between adjacent rings in agreement with more planar S_1 excited state. The energy of the $S_1 \leftarrow S_0$ electronic transition follows the HOMO−LUMO energy gap of each derivative. The overall shape of the absorption and fluorescence spectra suggests that a smaller distribution of conformers seems to be present in the S_1 state compared to that found in the ground state.

The insertion of methyl groups at the 3-position of each thiophene rings creates a twisting of the molecules which caused a blue-shift of the absorption band as well as a decrease of its absorption coefficient and an increase of its absorption bandwidth. Optimized geometries obtained from HF/6-31G* ab initio calculations are in good agreement with these experimental results. On the other hand, the fluorescence of both molecules (TFT and MTFMT) appears at the same wavelength. This strongly suggests that, after excitation, the first excited singlet state of MTFMT relaxes to a more planar conformation similar to that found for the unsubstituted molecule.

Addition of ester groups at both ends of the thiophene−fluorene oligomers induces a red-shift of the absorption and fluorescence bands. With the help of ab initio calculations, this behavior has been interpreted in terms of an increase of the conjugation length without any significant conformational changes. The spectral properties of the polymers are very close to those of their ester derivatives, showing that the triad units are well isolated in the polyester chain and that their molecular conformations remain about the same. However, judging

by their respective absorption and fluorescence bandwidths, the distribution of the conformers seems wider for the polyesters in their S_0 and S_1 electronic states.

Fluorescence quantum yield and lifetime of methyl-substituted derivatives are smaller than those of the unsubstituted molecules giving rise to a higher nonradiative decay rate constant for the former compounds. These results are interpreted in terms of an increase of the molecular flexibility for the methyl-substituted derivatives. Fluorescence quantum yield and lifetime of BTFBT are smaller than those of TFT giving rise to a higher nonradiative decay constant for the former molecule. On the basis of recent published papers in the literature on bithiophene derivatives, an enhancement of the intersystem crossing process caused by additional sulfur atoms in BTFBT might explain this behavior. On the other hand, the photophysics of the ester derivatives are mainly governed by smaller radiative properties giving rise to smaller fluorescence quantum yields. Finally, the fluorescence quantum yields of the polymers are smaller than the corresponding ester derivatives but the emission of the polyesters remains relatively intense. Thus, we believe that these polyesters may be used to develop organic blue light-emitting diodes. However it is important to mention here that TFTPE and MTFMTPE polyesters emit at about the same wavelength. To decrease the fluorescence wavelength of the polyesters, substituents creating more steric effects should be added to the thiophene−fluorene derivatives.

Acknowledgment. This work was supported by NSERC strategic and research grants. M.R. is grateful to NSERC for a fellowship.

References and Notes

(1) Garnier, F.; Hajlaoui, R.; Yassar, A.; Srivastava. *Science* **1994**, *265*, 1684.
(2) Drury, C.; Mutsaers, C.; Hart, C.; Matters, M.; de Leeuw, D. *Appl. Phys. Lett.* **1998**, *73*, 108.
(3) Pei, Q.; Yu; G.; Zhang, C.; Yang, Y. A.; Heeger, J. *Science* **1995**, *269*, 1086.
(4) Geiger, F.; Stoldt, M.; Schweizer, H.; Bauerle, P.; Umbach, E. *Adv. Mater.* **1993**, *5*, 922.
(5) Holmes, A. B.; Bradley, D. D. C.; Brown, A. R.; Burn, P. L.; Burroughes, J. H.; Friend, R. H.; Greenham, N. C.; Gymer, R. W.; Halliday, D. A.; Jackson, R. W.; Kraft, A.; Martens, J. H. F.; Pichler, K.; Samuel, I. D. W. *Synth. Met.* **1993**, *57*−*57*, 4031.
(6) Roth, S.; Graupner, W. *Synth. Met.* **1993**, *55*−*57*, 3623.
(7) Bauerle, P. *Adv. Mater.* **1993**, *5*, 879.
(8) Gustafsson, G.; Cao Y.; Treacy, G. M.; Klavetter, F.; Colaneri, C.; Heeger A. J. *Nature* **1992**, *357*, 477.
(9) Burns, P. L.; Holmes A. B.; Kraft, A.; Bradley, D. D. C.; Brown, A. R.; Friend R. H.; Gywer, R. W. *Nature* **1992**, *356*, 47.
(10) Burroughes, J. H.; Bradley D. D. C.; Brown, A. R.; Marks, R. N.; Mackay, K.; Friend, R. H.; Burns, P. L.; Holmes, A. B. *Nature* **1990**, *347*, 539.
(11) DiCésare, N.; Belletête, M.; Leclerc, M.; Durocher, G. *J. Phys. Chem. A* **1999**, *103*, 795.
(12) DiCésare, N.; Belletête, M.; Leclerc, M.; Durocher, G. *J. Phys. Chem. A* **1999**, *103*, 803.
(13) DiCésare, N.; Belletête, M.; Leclerc, M.; Durocher, G. *J. Phys. Chem. A* **1999**, *103*, 3864.
(14) Becker, R. S.; Seixas de Melo, J.; Maçanita, A. L.; Elisei, F. *J. Phys. Chem.* **1996**, *100*, 18683.
(15) Yassar, A.; Horowitz, G.; Valat, P.; Wintgens, V.; Hmyene, M.; Deloffre, F.; Srivastava, P.; Lang, P.; Garnier, F. *J. Phys. Chem.* **1995**, *99*, 9155.
(16) Egelhaaf, H.-J.; Bauerle, P.; Rauer, K.; Hoffman, V.; Oelkrug, D. *Synth. Met.* **1993**, *61*, 143.
(17) Egelhaaf, H.-J.; Bauerle, P.; Rauer, K.; Hoffman, V.; Oelkrug, D. *J. Mol. Struct.* **1993**, *293*, 249.
(18) Athouel, L.; Froyer, G.; Riou, M. T. *Synth. Met.* **1993**, *55*−*57*, 4734.
(19) Fichou, D.; Horowitz, G.; Xu, B.; Garnier, F. *Synth. Met.* **1992**, *48*, 167.
(20) DiCésare, N.; Belletête, M.; Donat-Bouillud, A.; Leclerc, M.; Durocher, G. *J. Lumin.* **1999**, *81*, 111.
(21) DiCésare, N.; Belletête, M.; Donat-Bouillud, A.; Leclerc, M.; Durocher, G. *Macromolecules* **1998**, *31*, 6289.
(22) Goldenberg, L. M.; Leclerc, M.; Donat-Bouillud, A.; Pearson, C.; Petty, M. C. *Thin Solid Films* **1998**, *327*, 715.
(23) Kreyenschmidt, M.; Klaerner, G.; Fuhrer, T.; Ashenhurst, J.; Karg, S.; Chen, W. D.; Lee, V. Y.; Scott, J. C.; Miller, R. D. *Macromolecules* **1998**, *31*, 1099.
(24) Ranger, M.; Rondeau, D.; Leclerc, M. *Macromolecules* **1997**, *30*, 7686.
(25) Pei, Q.; Yang, Y. *J. Am. Chem. Soc.* **1996**, *118*, 7416.
(26) Grell, M.; Bradley, D. D. C.; Inbasekaran, M.; Woo, E. P. *Adv. Mater.* **1997**, *9*, 798.
(27) Nijegorodov, N. I.; Downey, W. S.*J. Phys. Chem.* **1994**, *98*, 5639.
(28) Kauffman, J. M.; Litak, P. T.; Novinski, J. A.; Kelley, C. J.; Ghiorghis, A.; Qin, Y. *J. Fluoresc.* **1995**, *5*, 295.
(29) Belletête, M.; Ranger, M.; Beaupré, S.; Leclerc, M.; Durocher, G. *Chem. Phys. Lett.* **2000**, *316*, 101.
(30) Belletête, M.; Beaupré, S.; Bouchard, J.; Blondin, P.; Leclerc, M.; Durocher, G. *J. Phys. Chem. B.* **2000**, *104*, 9118.
(31) Coulson, D. R. *Inorg. Synth.* **1972**, *XIII*, 121.
(32) Ranger, M.; Leclerc, M. *J. Chem. Soc., Chem. Commun.* **1997**, 1597.
(33) Bäuerle, P.; Würthner, F.; Götz, G.; Effenberger, F. *Synthesis* **1993**, 1099.
(34) Barbarella, G.; Bongini, A.; Zambianchi, M. *Macromolecules* **1994**, *27*, 3039.
(35) Kellogg, R. M.; Schaap, A. P.; Harper, E. T.; Wynberg, H. *J. Org. Chem.* **1968**, *33*, 7, 2904.
(36) Beaupré, S.; Ranger, M.; Leclerc, M. *Macromol. Rapid. Commun.* **2000**, *21*, 1013.
(37) Eaton, D. F. *Pure Appl. Chem.* **1988**, *160*, 1107.
(38) Zelent, B.; Ganguly, T.; Farmer, L.; Gravel, D.; Durocher, G. *J. Photochem. Photobiol* **1991**, *56*, 165.
(39) Frisch, M. J.; Trucks, G. W.; Schlegel, H. B.; Scuseria, G. E.; Robb, M. A.; Cheeseman, J. R.; Zakrzewski, V. G.; Montgomery, J. A., Jr.; Stratmann, R. E.; Burant, J. C.; Dapprich, S.; Millam, J. M.; Daniels, A. D.; Kudin, K. N.; Strain, M. C.; Farkas, O.; Tomasi, J.; Barone, V.; Cossi, M.; Cammi, R.; Mennucci, B.; Pomelli, C.; Adamo, C.; Clifford, S.; Ochterski, J.; Petersson, G. A.; Ayala, P. Y.; Cui, Q.; Morokuma, K.; Malick, D. K.; Rabuck, A. D.; Raghavachari, K.; Foresman, J. B.; Cioslowski, J.; Ortiz, J. V.; Stefanov, B. B.; Liu, G.; Liashenko, A.; Piskorz, P.; Komaromi, I.; Gomperts, R.; Martin, R. L.; Fox, D. J.; Keith, T.; Al-Laham, M. A.; Peng, C. Y.; Nanayakkara, A.; Gonzalez, C.; Challacombe, M.; Gill, P. M. W.; Johnson, B.; Chen, W.; Wong, M. W.; Andres, J. L.; Gonzalez, C.; Head-Gordon, M.; Replogle, E. S.; Pople, J. A. Gaussian, Inc., Pittsburgh, PA, 1998.
(40) Ridley, J.; Zerner, M. C. *Theor. Chim. Acta* **1973**, *32*, 111.
(41) Forber, C.; Zerner, M. C. *J. Am. Chem. Soc.* **1985**, *107*, 5884.
(42) Blondin, P.; Bouchard, J.; Beaupré, S.; Belletête, M.; Durocher, G.; Leclerc, M. *Macromolecules* **2000**, *33*, 5874.
(43) Zhang, X.; Pitts, J. D.; Nadarajah, R.; Knee, J. L. *J. Chem. Phys.* **1997**, *107*, 8239.
(44) De Oliveira, M. A.; Duarte, H. A.; Pernaut, J.-M.; De Almeida, W. B. *J. Phys. Chem. A* **2000**, *104*, 8256.
(45) Becker, R. S.; Seixas De Malo, J.; Maçanita, A. L.; Elisei, F. *Pure Appl. Chem.* **1995**, *87*, 9.
(46) Rossi, R.; Ciofalo, M.; Carrita, A.; Ponterini, G. *J. Photochem. Photobiol. A: Chem.* **1993**, *70*, 59.
(47) Lüssen, G.; Festag, R.; Greiner, A.; Schmidt, C.; Unterlechner, C.; Heitz, W.; Wendorff, J. H.; Hopmeier, M.; Feldman, J. *Adv. Mater.* **1995**, *7*, 923.

MA001042A